Direct-potential-fit analyses yield improved empirical potentials for the ground $X\,^1\Sigma_g^+$ state of Be_2

Vladimir V. Meshkov,[1] Andrey V. Stolyarov,[1,a)] Michael C. Heaven,[2,b)] Carl Haugen,[3] and Robert J. LeRoy[3,c)]
[1]*Department of Chemistry, Lomonosov Moscow State University, Leninskie gory 1/3, 119991 Moscow, Russia*
[2]*Department of Chemistry, Emory University, Atlanta, Georgia 30322, USA*
[3]*Guelph-Waterloo Centre for Graduate Work in Chemistry and Biochemistry, University of Waterloo, Waterloo, Ontario N2L 3G1, Canada*

(Received 14 November 2013; accepted 25 January 2014; published online 14 February 2014)

We have performed new direct-potential-fit (DPF) analyses of the rotationally resolved $A\,^1\Pi_u(v' = 2, 3; J' = 1, 2) \rightarrow X\,^1\Sigma_g^+(v'' \in [0, 11]; J'' \in [0, 3])$ stimulated emission pumping spectra of Be_2 [J. M. Merritt, V. E. Bondybey, and M. C. Heaven, Science **324**, 1548 (2009)] using two quite different analytical potential energy functions that incorporate the correct theoretically known long-range behaviour in different ways. These functions are: the damped Morse/long-range potential [R. J. Le Roy, C. C. Haugen, J. Tao, and H. Li, Mol. Phys. **109**, 435 (2011)], and the Chebyshev polynomial expansion potential [L. Busevica, I. Klincare, O. Nikolayeva, M. Tamanis, R. Ferber, V. V. Meshkov, E. A. Pazyuk, and A. V. Stolyarov, J. Chem. Phys. **134**, 104307 (2011)]. In contrast with the expanded Morse oscillator potential determined in the original DPF analysis of Merritt *et al.* [Science **324**, 1548 (2009)], both of these functions unambiguously support the existence of the $v'' = 11$ last vibrational levels which is bound by only $\sim$0.5 cm^{-1}, and they give equivalent, essentially exact predictions for this level when using the original data set which ended at $v'' = 10$. These empirical potentials predict an equilibrium distance of $r_e = 2.445(5)$ Å and a well depth of $\mathfrak{D}_e = 934.9(0.4)$ cm^{-1}, values which agree (within the uncertainties) with the best *ab initio* estimates of 2.444(10) Å and 935(10) cm^{-1}, respectively [J. Koput, Phys. Chem. Chem. Phys. **13**, 20311 (2011)]. © *2014 AIP Publishing LLC*. [http://dx.doi.org/10.1063/1.4864355]

I. INTRODUCTION

The beryllium dimer has long presented a challenge, because in spite of the fact that it contains only eight electrons, the unusual nature of its bonding long made its quantitative description difficult for theory,[1–9] while the fact that metallic beryllium is refractory (having a low vapour pressure, even at high temperatures) and that beryllium-containing compounds are very toxic, made experiments with it very difficult. However, in recent work Merritt *et al.*[10] reported spectra which sample most of the beryllium dimer potential well, and performed an analysis which determined estimates of the bond dissociation energy $\mathfrak{D}_e$ and the equilibrium distance r_e by using a direct fit to those data to determine an "Expanded Morse Oscillator" (EMO) potential energy function:[11]

$$V_{\rm EMO}(r) = \mathfrak{D}_e\,(1 - \exp\{-\beta_{\rm EMO}(r)\cdot(r - r_e)\})^2\,, \qquad (1)$$

which has the form of a Morse potential with an exponential tail and a distance-dependent exponent coefficient

$$\beta_{\rm EMO}(r) = \sum_{i=0}^{N_\beta} \beta_i^{\rm EMO}\cdot y_p^{\rm eq}(r)^i\,, \qquad (2)$$

that is expressed as a simple power series in the dimensionless radial variable

$$y_p^{\rm eq}(r) = \frac{r^p - r_e^p}{r^p + r_e^p}\,. \qquad (3)$$

The object of the present study is to determine improved experimental estimates of the fundamental properties of the ground $X\,^1\Sigma_g^+$ state of Be_2, and to examine how the quality of the molecular information determined in this type of analysis depends of the quality of the model used for the potential energy function. In particular, we show that performing such an analysis using two different types of model potentials possessing the physically justified inverse-power-sum long-range tail[12] confirms the fact that this species actually has one more bound level[7] than is supported by the empirical EMO potential of Merritt *et al.*, or had been observed in the data set on which it was based. The values of the equilibrium distance and well depth obtained from the present analyses do not depend significantly on whether or not the new data subsequently obtained for the experimentally elusive $v = 11$ vibrational level are included in the analysis. Figure 1 shows that our two new fitted potentials (Chebyshev polynomial expansion (CPE) and Morse/long-range (MLR[ab]) curves) are essentially identical to each other (on this scale) and in very good agreement with recent *ab initio* results (points) for this system.

a)Electronic mail: avstol@phys.chem.msu.ru
b)Electronic mail: heaven@euch4e.chem.emory.edu
c)Electronic mail: leroy@uwaterloo.ca

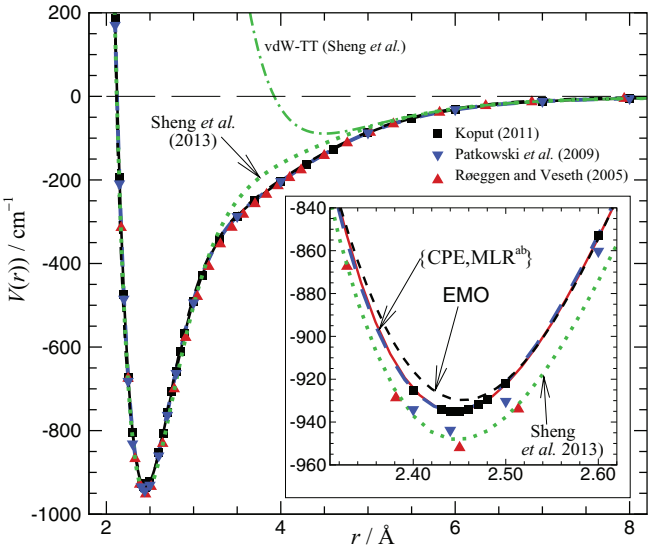

FIG. 1. Overview of the Be_2 ground $X\,^1\Sigma_g^+$ state potential showing the *ab initio* points from Refs. 3, 7, and 8, the EMO potential of Merritt *et al.*[10] (dashed black curve), the present recommended empirical MLR^{ab} and CPE potentials (solid black and thick blue dashed curves), and both the full analytic potential of Sheng *et al.*[9] (green dotted curve) and its "van der Waals" component (green dashed-dotted curve). Inset: expanded view of the potential minimum region.

II. DIRECT-POTENTIAL-FIT (DPF) ANALYSIS

A. Outline of the DPF procedure

In recent years it has become increasingly common to analyze diatomic molecule spectroscopic data by performing "direct potential fits" (DPFs), in which observed transition energies are compared with eigenvalue differences calculated from an effective radial Schrödinger equation

$$\left(-\frac{1}{2\mu}\frac{d^2}{dr^2} + V(r;\alpha_1,\ldots,\alpha_n) + \frac{J(J+1)}{2\mu r^2} - E_{vJ}\right) \times |v^J\rangle = 0, \tag{4}$$

based on some parameterized, analytic, mass-invariant potential energy function $V(r;\alpha_1,\ldots,\alpha_n)$.[13–32] Here, $\alpha_1, \ldots, \alpha_n$ are parameters defining the potential, r is the internuclear distance, and E_{vJ} is the ro-vibronic energy. This DPF approach[29] is at the core of the present work.

We have performed DPF analyses using two quite different analytical potential energy functions that incorporate the correct theoretically known long-range behaviour in very different ways, namely: the damped MLR potential[30] and the CPE potential.[31] These functions are described in detail in Subsection II B. Our recommended empirical potential functions $V(r;\alpha_1,\ldots,\alpha_n)$ for the ground $X\,^1\Sigma_g^+$ state of Be_2 were determined by application of weighted non-linear least-squares fitting procedures that minimizes the quantity:[29]

$$\chi^2_{\rm expt} = \sum_{j=1}^{N_{\rm expt}} \left(\frac{\nu_j^{\rm expt} - \nu_j^{\rm calc}}{\sigma_j^{\rm expt}}\right)^2, \tag{5}$$

in which $\nu_j^{\rm expt}$ are the experimental transition energies, $\nu_j^{\rm calc} = \nu_j^{\rm calc}(\{\alpha_i\}) \equiv E^A_{v'J'} - E^X_{v''J''}$ are the values of these quantities calculated from the model, and $\sigma_j^{\rm expt}$ is the experimental uncertainty in datum-j.

The experimental data set for the $X\,^1\Sigma_g^+$ state of Be_2 used in the present work consists of 73 $R(1)$, $P(2)$, $P(3)$, and $Q(1)$ lines emitted from two rotational sublevels of each of the $v' = 2$ and 3 vibrational levels of the $A\,^1\Pi_u$ state into the $v'' = 0, \ldots, 11$ levels of the ground $X\,^1\Sigma_g^+$ state (see the supplementary material[33]). They were observed in stimulated emission pumping (SEP) experiments performed on Be_2 that was formed in the gas phase with a rotational temperature of 2.0 K.[10] The reported uncertainties in these data were $\sigma_j^{\rm expt} = 0.1$ and 0.2 $\rm cm^{-1}$ for transitions originating in $v' = 2$ and 3, respectively. In our analyses, the energy levels of the $A\,^1\Pi_u$ state were usually represented by four independent fitted term values $E^A_{v'J'}$, and the Λ-doubling effect in the doubly degenerate levels of the upper state was neglected. Although it would be possible to fit to separate e' and f' term values for each A' state v', J' level, the small size of the data set and the fact that the RMS discrepancies from the present fits are already (on average) half the experimental uncertainties indicate that little would be gained. The energy levels of the ground $X\,^1\Sigma_g^+$ state $E^X_{v''J''}$ were calculated from Eq. (4) while using one of our parameterized analytic potential energy functions. This data set extended beyond that available to Merritt *et al.*[10] because it included laser-induced fluorescence transitions from the lowest level ($v'' = 0$, new data recorded in 2009) and SEP transitions to the very highest ($v'' = 11$) vibrational level.[35]

The radial equation (4) was solved numerically on the semi-interval $r \in [1.5, +\infty)$ Å, either by means of an analytical mapping procedure,[34] or by a conventional radial propagation procedure.[36] In solving the radial equation (4), we set $\frac{1}{2\mu} \equiv \frac{16.85762920}{\mu}$ [amu Å^2 cm^{-1}] to define the units of length and energy as Å and $\rm cm^{-1}$, respectively,[37] where $\mu = 4.50609110$ is the molecular reduced mass of $^9Be_2$ in amu.[38]

In order to ensure that the repulsive walls of these empirical potentials would extrapolate sensibly on the interval $r \lesssim 2.1$ Å where the experimental data provide no information, some of the fits incorporated a few ($N_{\rm ab} = 5$) *ab initio* potential function values $V_{\rm ab}(r_j)$ taken from Ref. 3 as "data" in the fits. In particular, rather than simply seeking the minimum of the quantity $\chi^2_{\rm expt}$ from Eq. (5), these fits minimize the sum $\chi^2_{\rm expt} + \chi^2_{\rm ab}$, in which

$$\chi^2_{\rm ab} \equiv \sum_{j=1}^{N_{\rm ab}} \left(\frac{V_{\rm ab}(r_j) - V(r_j;\alpha_1,\ldots,\alpha_n)}{\sigma_{\rm ab}}\right)^2. \tag{6}$$

In these fits, the uncertainties $\sigma_{\rm ab}$ in the *ab initio* points were set at 100 $\rm cm^{-1}$, a value that was estimated by comparing the *ab initio* potential energy curves (PECs) from different sources.[1,3,4,7,8] Figure 2 illustrates the short-range behaviour of empirical potentials determined by minimizing $\chi^2_{\rm expt}$ alone (thin dashed curves), with those determined by minimizing the sum $\chi^2_{\rm expt} + \chi^2_{\rm ab}$ (solid and thick dashed curves).

While the MLR potential function explicitly includes the known values[12] of the long-range potential coefficients $C_n^{\rm ab}$ in the potential form, in the CPE potential function, the values of

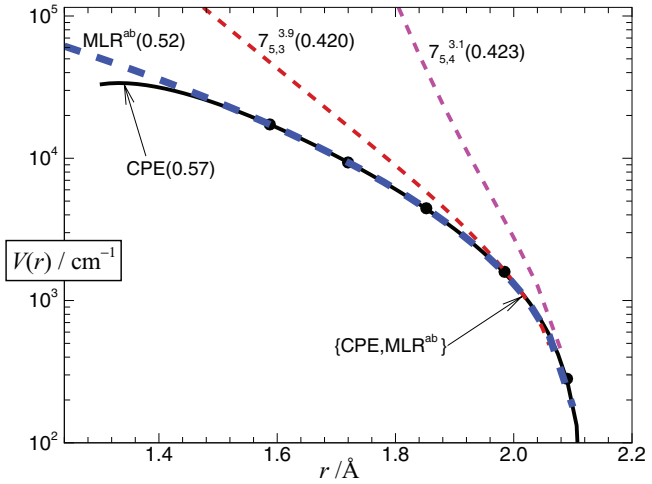

FIG. 2. Plot showing the short-range behaviour of some of our empirical MLR and CPE potentials, and the selected set of five *ab initio* points (round black points) used as additional data in some of the fits (see text). The labels for the MLR curves determined purely from experimental data are $N^{r_{\rm ref}}_{p,q}(\overline{dd})$, in which $N = N_\beta$ and $\overline{dd}$ is the dimensionless RMS deviation for the fit to that model. The MLR$^{\rm ab}$ and CPE curves are the recommended empirical potentials determined from fits that also treated 5 selected *ab initio* points as data; see Tables II and III.

the leading long-range C_n coefficients are defined as functions of the coefficients c_k of the polynomial expansion (see Sec. II B 2). Thus, in order to force the long-range behaviour of the CPE potential to conform as closely as possible to that implied by the *ab initio* dispersion coefficients,[12] the expansion coefficients $\{\alpha_k\}$ were constrained during the fit by minimization of the functional $\chi^2_{\rm tot} \equiv \chi^2_{\rm expt} + \chi^2_{\rm ab} + \chi^2_{C_n}$, where

$$\chi^2_{C_n} = \sum_{n=6,8,10} \left(\frac{C_n^{ab} - C_n^{\rm CPE}}{\sigma_n} \right)^2, \tag{7}$$

in which the dispersion coefficient $C_n^{\rm CPE}$ were defined by Eqs. (22)–(24) of Sec. II B 2. The *ab initio* values $C_n^{\rm ab}$ used here are those generated by Porsev and Derevianko from their highly accurate calculation of the dynamic polarizabilities of atomic Be.[12] These quantities, with their uncertainties σ_n shown in parentheses, are presented in the middle column of Table I.

In fits to the CPE potential, minimization of $\chi^2_{\rm tot}$ with respect to the expansion parameters was performed using the robust Levenberg-Marquardt algorithm,[39,40] while the minimization of $\chi^2_{\rm expt}$ or $\chi^2_{\rm expt} + \chi^2_{\rm ab}$ for the MLR model potential was performed using a simple iterative "steepest descents" procedure.[37] In both cases, the diagonal Hellmann-Feynman theorem

$$\frac{\partial E_{vJ}}{\partial \alpha_k} = \left\langle v^J \left| \frac{\partial V}{\partial \alpha_k} \right| v^J \right\rangle_r \tag{8}$$

was used to calculate the required partial derivatives of the simulated transition energies with respect to the potential function parameters. In both cases, the initial values of the fitting parameters required to start the non-linear minimization procedure were obtained by performing fits of our potential function forms to the point-wise *ab initio* potential.[3,4,8]

Estimates of the uncertainties $u\{V(r)\}$ in values of the final fitted potentials were obtained by combining the covariance matrices $\mathbf{C}_{k,l}$ and uncertainties in the fitted parameters $u\{\alpha_i\}$ yielded by the fits, with the readily generated partial derivatives $\partial V/\partial \alpha_j$, using the expression[41]

$$u\{V(r)\} \approx \sqrt{\sum_{k=1}^{n}\sum_{l=1}^{n} \left(u\{\alpha_k\} \cdot \frac{\partial V}{\partial \alpha_k} \right) \left(u\{\alpha_l\} \cdot \frac{\partial V}{\partial \alpha_l} \right) \mathbf{C}_{k,l}}. \tag{9}$$

TABLE I. Comparison of theoretical dispersion coefficients $C_n^{\rm ab}$ for a pair of interacting ground-state ($2\,^1S$) Be atoms (with their uncertainties σ_n in parentheses) with empirical values determined from the fitted CPE potential using Eqs. (22)–(24).

	Ab initio[12]	CPE
$C_6(10^6{\rm cm}^{-1}{\rm Å}^6)$	1.0313 (0.0144)	1.0313
$C_8(10^7{\rm cm}^{-1}{\rm Å}^8)$	1.3806 (0.0081)	1.3804
$C_{10}(10^8{\rm cm}^{-1}{\rm Å}^{10})$	1.9058 (0.0461)	1.9117

B. The potential function models

To minimize the effect of model-dependence on our estimates of the key molecular properties being determined, the adiabatic potential of ground-state Be_2 was represented using two very different types of analytic functions, both of which account properly for its theoretically known inverse-power-sum long-range behaviour:

$$V(r \to +\infty) \to \mathfrak{D} - \sum_{n=6,8,10,\ldots} \frac{C_n}{r^n}, \tag{10}$$

in which $\mathfrak{D}$ is the absolute energy at the dissociation limit. The values of the leading dispersion coefficients C_6, C_8, and C_{10} used here are the $C_n^{\rm ab}$ values in column 1 of Table I. The dispersion potential of Eq. (10) is expected to come to dominate the interaction at distances beyond what is called the "Le Roy radius":[42]

$$r_{\rm LR} = 4\sqrt{\langle r^2_{\rm el}\rangle^{\rm Be}} \approx 6.2\,{\rm Å}, \tag{11}$$

in which $\langle r^2_{\rm el}\rangle^{\rm Be}$ is the expectation value of the square of the radius of the electrons in the valence shell of atomic beryllium.[43] Figure 3 shows that this distance is close to the outer turning point of the third-highest observed level, $r_{\rm out}(v = 9) \approx 6.5$ Å.

1. The Morse-long range (MLR) function

The MLR potential energy function has the form

$$V_{\rm MLR}(r) = \mathfrak{D}_e \left(1 - \frac{u_{\rm LR}(r)}{u_{\rm LR}(r_e)} \exp\left\{ -\beta(r) \cdot y_p^{\rm eq}(r) \right\} \right)^2, \tag{12}$$

in which $\mathfrak{D}_e$ is the well depth, r_e is the equilibrium internuclear distance, $u_{\rm LR}(r)$ defines the limiting long-range behaviour of the potential and $u_{\rm LR}(r_e)$ is the value of that function at $r = r_e$. The radial variable $y_p^{\rm eq}$ in the exponent of

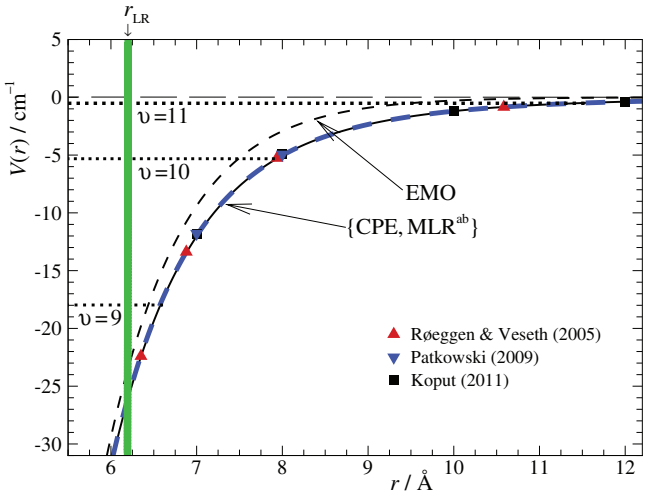

FIG. 3. Long-range behaviour of the present recommended empirical MLR^{ab} (dashed blue curve) and CPE (solid black curve) potentials compared with their EMO analog[10] and available *ab initio* points.[3,7,8] The Le Roy radius r_{LR} was evaluated from Eq. (11).

Eq. (12) is given by Eq. (3), while the exponent coefficient function

$$\beta(r) = y_p^{\rm ref}(r)\,\beta_\infty + \left[1 - y_p^{\rm ref}(r)\right]\sum_{i=0}^{N_\beta}\beta_i\,[y_q^{\rm ref}(r)]^i \quad (13)$$

is defined in terms of two radial variables that are similar to $y_p^{\rm eq}$, but are defined with respect to a different expansion centre ($r_{\rm ref}$), and involve two separate powers, p and q:[28,30,37]

$$y_p^{\rm ref}(r) = \frac{r^p - r_{\rm ref}^p}{r^p + r_{\rm ref}^p} \quad \text{and} \quad y_q^{\rm ref}(r) = \frac{r^q - r_{\rm ref}^q}{r^q + r_{\rm ref}^q}. \quad (14)$$

The above definition of the function $\beta(r)$ means that

$$\lim_{r\to\infty}\beta(r) \equiv \beta_\infty = \ln[2\mathfrak{D}_e/u_{\rm LR}(r_e)]. \quad (15)$$

Then, since the three dimensionless radial variables of Eqs. (3) and (14) all approach unity as $r \to \infty$, at long range the MLR potential takes on the form

$$V_{\rm MLR}(r) \simeq \mathfrak{D}_e - u_{\rm LR}(r). \quad (16)$$

As a generalization of Eq. (10), the long-range potential may include "damping functions" $D_n(r)$ that take account of the weakening of dispersion forces at shorter distances due to overlap of the electronic wavefunctions of the two atoms:

$$u_{\rm LR}(r) = \sum_{n=6,8,10} D_n(r)\frac{C_n}{r^n}. \quad (17)$$

These functions also tend to stabilize the behaviour of the repulsive wall at very short distances.[30] Following the recommendation of Ref. 30, the damping functions used here are the "$s = -1$" version of the generalized Douketis form:[30]

$$D_n(r) = \left(1 - \exp\left\{-\frac{3.3(\rho r)}{n} - \frac{0.423(\rho r)^2}{n^{1/2}}\right\}\right)^{n-1}, \quad (18)$$

in which the dimensionless, system-dependent mapping parameter $\rho = (I_P^{\rm Be}/I_P^{\rm H})^{2/3} = 0.78$ is defined by the ratio of the ionization potentials of the Be and H atoms.[43] Note that the MLR function explicitly incorporates the *ab initio* C_6, C_8, and C_{10} values of Table I.

2. Chebyshev polynomial expansion (CPE) function

The second type of potential function form considered here is the "Chebyshev polynomial expansion" or CPE function. It is defined continuously on the semi-interval $r \in [r_{\rm min}, +\infty)$ by the analytical function:[31]

$$V_{\rm CPE}(r) = -\frac{\sum_{k=0}^{N_c} c_k\,T_k(y_p)}{1 + (r/r_{\rm ref})^n}, \quad (19)$$

in which n is a positive integer whose value is chosen to enable $V_{\rm CPE}(r)$ to have the desired long-range behaviour. The functions $T_k(y)$ are the Chebyshev polynomials of the first kind,[44] defined in terms of the reduced variable $y_p(r) \in [-1, 1]$:

$$y_p(r; r_{\rm min}, r_{\rm ref}) = \frac{r^p - r_{\rm ref}^p}{r^p + r_{\rm ref}^p - 2{r_{\rm min}}^p}, \quad (20)$$

in which p is a small positive integer whose value is also chosen to enable $V_{\rm CPE}(r)$ to have the desired long-range behaviour. Parameter $r_{\rm ref}$ is a reference distance chosen as the expansion centre, and $r_{\rm min}$ is the smaller of the inner end of the radial integration range or the smallest distance associated with the *ab initio* data points included in the analysis ($r_{\rm ref} > r_{\rm min} \geq 0$).[45]

A key property of this function is the fact that it is a linear function of its expansion parameters, $\{c_k\}$. As a result, the partial derivatives of the calculated energies with respect to any of the fitting parameters c_k that are required for the fit (see Eq. (8)),

$$\frac{\partial E_{vJ}}{\partial c_k} = \left\langle v^J \left| \frac{-T_k}{1 + (r/r_{\rm ref})^n} \right| v^J \right\rangle_r, \quad (21)$$

do not depend explicitly on *any* of these expansion parameters. Thus, a fit to the CPE potential form is only non-linear in "second-order," because of the dependence of the radial vibrational wavefunctions $|v^J\rangle$ on the expansion parameters $\{c_k\}$. This is markedly different from the situation for the MLR potential, for which the analogous partial derivatives depend explicitly on *all* of the potential function parameters. This means that fits using the MLR form will tend to require more iterative cycles before they converge fully.

It may also be shown that if the fixed integers n in Eq. (19) and p in the definition of the expansion variable by Eq. (20) are given the values $n = 6$ and $p = 2$, then at long range, this CPE function (19) takes on the theoretically predicted long-range form of Eq. (10), with the three leading dispersion coefficients being defined by the expressions

$$C_6^{\rm CPE} = r_{\rm ref}^6\left[\sum_{k=0}^{N_c} c_k\right], \quad (22)$$

$$C_8^{\rm CPE} = -2\Delta r^2 r_{\rm ref}^6\left[\sum_{k=0}^{N_c} k^2\,c_k\right], \quad (23)$$

$$C_{10}^{\mathrm{CPE}} = \frac{2}{3}\left[\Delta r^2\right]^2 r_{\mathrm{ref}}^6 \times \left\{\sum_{k=0}^{N_c} k^4 c_k + \left[2 - 3\left(\frac{r_{\mathrm{min}}^2}{\Delta r^2}\right)\right]\sum_{k=0}^{N_c} k^2 c_k\right\}, \quad (24)$$

in which $\Delta r^2 \equiv r_{\mathrm{ref}}^2 - r_{\mathrm{min}}^2$. It is the use of these expressions in Eq. (7) that causes fitted CPE potentials to have the desired long-range form.

III. RESULTS AND DISCUSSION

The analyses using both potential forms began with a "manual" search for the optimum value of the expansion centre distance r_{ref}, and for the smallest expansion polynomial order (N_β in Eq. (12) or N_c in Eq. (19)), for which the converged fit gave a minimum of the dimensionless root-mean-square deviation $\overline{dd} \equiv \sqrt{\chi^2/N_{\mathrm{data}}}$. Fits of MLR potentials to the experimental data alone indicated that the optimum MLR model was one with $N_\beta = 7$, $\{p, q\} = \{5, 3\}$, and $r_{\mathrm{ref}} = 3.9$ Å, for which $\overline{dd}_{\mathrm{expt}} = 0.42$ (for details see Figure App-1 of the supplementary material[33]). Unfortunately, Fig. 2 shows that the short-range extrapolation behaviour of this MLR potential (red dashed curve) is not fully satisfactory. Although it passes through the first two (largest-r) of our selected repulsive-wall *ab initio* points, it provides poor predictions for the others. Hence, although it is not effectively required by the model (as it is for CPE functions), our MLR analysis was extended by repeating these fits while including the five selected *ab initio* points as data in the analysis (i.e., by minimizing $\chi^2_{\mathrm{expt}} + \chi^2_{\mathrm{ab}}$ rather than just χ^2_{expt}). The optimum model determined in this manner is an MLR$^{\mathrm{ab}}$ function with $N_\beta = 6$, $\{p, q\} = \{5, 4\}$, and $r_{\mathrm{ref}} = 3.4$ Å shown as thick blue short-dashed curves in Figs. 1–3. This is our recommended MLR model for this system. Its somewhat poorer $\overline{dd}_{\mathrm{expt}} = 0.51$ value (*vs.* 0.42 above) is the cost of requiring the fit to accommodate simultaneously the experimental and *ab initio* data.

With their expansion variables defined by the integers $p = 2$ and $n = 6$, fits of CPE potentials that minimized $\chi^2_{\mathrm{tot}} \equiv \chi^2_{\mathrm{expt}} + \chi^2_{\mathrm{ab}} + \chi^2_{C_n}$ were performed for polynomial orders $N_c = 11$–13 and r_{ref} values ranging from 2.4 to 5.1 Å. This led to the model with $N_c = 12$ and $r_{\mathrm{ref}} = 3.2$ Å being chosen as the recommended CPE potential. Figure App-2 of the supplementary material[33] provides details of this optimization procedures, and Table I shows that the C_n values of the CPE potential that was determined in this way are in excellent agreement with the *ab initio* values. Figure 3 shows that our two fitted potential are in good agreement with one another and with the *ab initio* results at long range.

The parameters defining the recommended MLR$^{\mathrm{ab}}$ and CPE potentials are presented in Tables II and III, respectively. Their values were rounded off using the type of procedure described in Ref. 41, which minimizes the number of digits presented without significantly reducing the precision of the representation of the data. In the present case, this rounding increased the values of $\overline{dd}$ by less than 0.25%. On the scales of Figs. 1–3 our two recommended PECs are virtually superimposed, except at very small internuclear distances (see Fig. 2) where the extrapolated CPE potential turns over in the region past the last (smallest-r) *ab initio* data point. However, Fig. 4 shows that even there, the differences between these functions lie within the range of the uncertainties predicted using Eq. (9). Figure 3 also shows the significantly different shape of the long-range tail of the empirical "EMO" potential yielded by the original analysis of Merritt *et al.*[10] Our two recommended PECs both provide excellent levels of accuracy

TABLE II. Parameters defining the recommended MLR$^{\mathrm{ab}}$ potential determined from a simultaneous DPF fit to the 73 experimental transition energies of Merritt *et al.*[10] and Heaven[35] and the five selected *ab initio* points[3] at $r < 2.1$ Å (see the supplementary material[33]). The 3 dispersion coefficients were fixed at the *ab initio* values in Table I, and the damping functions were defined by Eq. (18) with $\rho = 0.78$.

Fitted	
$\mathfrak{D}_e(\mathrm{cm}^{-1})$	934.8(3)
r_e(Å)	2.445(5)
β_0	0.55203
β_1	−0.193
β_2	−1.306
β_3	0.67
β_4	0.88
β_5	−1.615
β_6	−1.22
Fixed	
$\{p, q\}$	$\{5, 4\}$
r_{ref} (Å)	3.4
Derived	
$\mathfrak{D}_0(\mathrm{cm}^{-1})$	808.18
β_∞	−0.6764134752057

TABLE III. Expansion coefficients $\{c_k\}$ (in units cm^{-1}) defining the recommended CPE potential. The long-range behaviour was constrained by Eqs. (22)–(24) to agree with that implied the *ab initio* dispersion coefficients in Table I.

Fitted	
c_0	3253.820
c_1	−8032.983
c_2	6254.785
c_3	−4002.789
c_4	2257.260
c_5	−711.360
c_6	−16.487
c_7	44.198
c_8	−44.912
c_9	51.794
c_{10}	−23.636
c_{11}	18.620
c_{12}	−8.828
Fixed	
$\{n, p\}$	$\{6, 2\}$
r_{min} (Å)	1.5
r_{ref} (Å)	3.2
Derived	
r_e(Å)	2.445(3)
$\mathfrak{D}_e(\mathrm{cm}^{-1})$	935.0(3)
$\mathfrak{D}_0(\mathrm{cm}^{-1})$	808.20

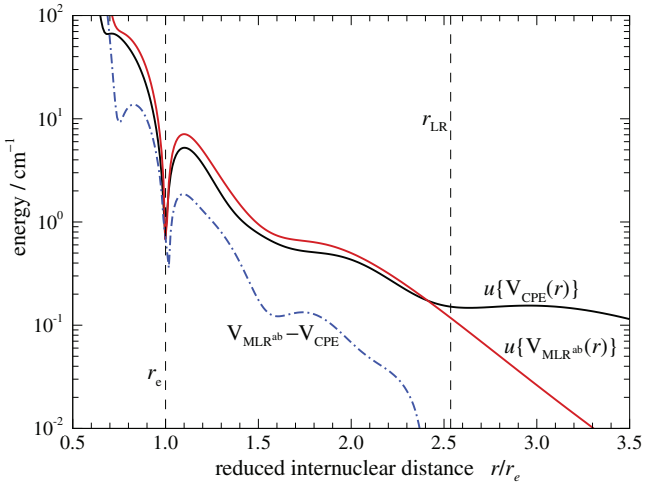

FIG. 4. Comparison of the confidence interval uncertainties $u\{V(r)\}$ (on a logarithmic scale) for our fitted MLR^{ab} and CPE potentials predicted using Eq. (9) (solid black and red curves) with the difference between these two potentials (dotted-dotted-dashed blue curve). The local minima of the solid curves near r_e correspond to our well depth uncertainties of ∼0.3 cm^{-1}.

with regard to their representation of the experimental data, yielding $\overline{dd}_{\rm expt}({\rm MLR^{ab}}) = 0.52$ and $\overline{dd}_{\rm expt}({\rm CPE}) = 0.57$, respectively. The fact that all of our optimized-model $\overline{dd}_{\rm expt}$ values are significantly less then 1 suggests that the reported uncertainties of the experimental data $\sigma_j^{expt} = 0.1$–0.2 cm^{-1} were overestimated.

The original SEP data set of Merritt *et al.* only included direct observation of levels $v'' = 1$–10, and their fitted EMO potential function did not support the existence of $v'' = 11$. However, subsequent *ab initio* calculations of Patkowski *et al.*[7] and Koput[8] both yielded potentials that supported the existence of a $v'' = 11$ level, for the former, bound by approximately 0.4 cm^{-1}. The present work shows that an empirical analysis of the original experimental data using more sophisticated model potentials that incorporate the correct theoretically known[12] long-range behaviour clearly predict the existence of a $v'' = 11$ level bound by 0.52 cm^{-1}. Moreover, a recent re-examination of the SEP spectra[35] has now led to assignment of additional transitions that provide the first direct observation of $v'' = 11$. However, adding these lines to the data set did not affect significantly the present extrapolation to the asymptote (see Fig. Ap-3).

Selected properties of our two recommended potentials are compared with those of the EMO potential of Merritt *et al.*[10] and with results of other workers in Table IV. The "EMO (present)" results seen there were obtained from a new independent fit to the same data set used for the CPE and MLR^{ab} fits (omitting the $v'' = 11$ data). The factor of three difference with the $\overline{dd}$ value for the 2009 EMO potential reflects the fact that the original analysis was based on an early version of the data set that had reduced the ∼70 electronic transitions to 32 pseudo IR and pseudo MW data. Nonetheless, these results show that our two new potentials agree well with each other and with the EMO analysis of Merritt *et al.*[10] with regard to the value of the equilibrium internuclear distance r_e and the fundamental vibrational spacing $\Delta G_{1/2}$. The differences between the present $\mathfrak{D}_0$ values and those of the two EMO potentials reflect the improved extrapolation to the dissociation limit provided by our CPE and MLR^{ab} potential function models, as is illustrated by their different binding energies for $v'' = 10$, which is the highest bound level supported by the EMO potentials. However, a larger contribution (3.5–3.7 cm^{-1}) to the differences in their $\mathfrak{D}_e$ values comes from the different estimate of the zero-point energy. The fact that the values of this quantity yielded by our two very different models are in close agreement with each other (126.6 *vs.* 126.8 cm^{-1}) and with that implied by the recent *ab initio* potential of Koput[8] (126.9 cm^{-1}), and that our quality of fit is 20%–40% better than that obtained from the present fit to an

TABLE IV. Comparison of key properties of our two fitted potentials with those obtained in earlier work. Energies have units cm^{-1} and lengths are in Å, and $E_b(v) \equiv \mathfrak{D}_e - G(v)$.

Source	$\mathfrak{D}_e$	$\mathfrak{D}_0$	r_e	$\overline{dd}_{\rm expt}$	$\Delta G_{1/2}$	$E_b(10)$	$E_b(11)$	a_S
Empirical								
Bondybey[47]	790(30)	…	…	…	223.4	…	…	…
Martin[1]	944(25)	816.1	2.440	…	223.7			
EMO[10]	929.7(20)	806.53	2.4536	2.40	222.6	3.12	…	5.15
EMO (present)	929.6(3)	806.97	2.512(22)	0.71	222.9	3.17	…	4.87
MLR^{ab} (present)	934.8(3)	808.16	2.445(5)	0.51	222.92	5.32	0.518	0.91(40)
CPE (present)	935.0(3)	808.20	2.445(3)	0.57	222.92	5.36	0.521	0.77(35)
Ab initio								
Gdanitz[2]	898(8)	…	2.44	…	217.8	3.20	0.30	…
Røeggen[3]	945(15)	…	2.452	…	221.7	…	…	−6.0[5]
Patkowski[6]	938(15)	…	2.44					
Jamieson[5]	837.1	713.1	2.4485	…	214.4	1.73	…	28.6
Koput[8]	935(10)	808.1	2.444(3)	…	223.1			
Sheng[9]	948.3	824.9	2.448	132.1	220.0	2.65	0.08	…
Morphed *ab initio*								
Spirko[4]	922.9	…	2.438	…	223.3			
Patkowski[7]	934.6	807.42	2.438	(0.4)[7]	222.6	4.92	0.42	…

EMO potential, and 4–5 times better than that associated with the EMO potential of Merritt *et al.*[10] lead us to prefer the $\mathfrak{D}_e$ values implied by the present recommended potential energy functions. However, this remains a question regarding which future theoretical work could be decisive.

As a test of the stability of the present results, fits were also performed in which the spectroscopic data set was truncated at vibrational level $v''_{\max} < 11$. For $v''_{\max} = 10$, 9, and 8, the resulting values of $\mathfrak{D}_e$ and r_e all agreed with the final recommended $v''_{\max} = 11$ results (see Tables II–IV) within their uncertainties, while the a_s values for the $v''_{\max} = 10$ MLR^{ab} and CPE potentials differ from those in Table IV by less than the difference between them (see Fig. App-3 of the supplementary material[33]). This gives us confidence in the reliability of the present estimates of these properties, and of our model potentials for this system.

Table IV also shows that the much earlier work of Bondybey[47] gave a good estimate of the fundamental vibrational level spacing, and that the most recent *ab initio* potentials for this system also provided good estimates of most properties of this system. However, the scattering lengths a_S calculated from the current potentials differ significantly from estimate based on *ab initio* potentials.[3,5,46] Overall, our two quite different fitted analytic potentials are in good agreement with regard to all discussed properties of this system. In particular, both of our empirical potentials unambiguously support the morphed Patkowski *et al.*[7] model's prediction of the existence of a $v''_{\max} = 11$ vibrational level that is bound (in our case) by ca. 0.52 cm^{-1}.

The fitted values of the energies of the $A\,^1\Pi_u(v' = 2, 3; J' = 1, 2)$ levels that comprise the origins of the observed SEP progressions progression are presented in Table V. It is clear again that the results obtained using the two different potential function forms are equivalent, within the uncertainties. The $T_{v'}$ and $B_{v'}$ shown in columns 4 and 5 of Table V were obtained from a separate MLR^{ab} fit in which those term values were represented by the traditional "band constant" expression: $E_{v'J'} = T_{v'} + B_{v'}[J'(J'+1)]$. Full listings of the experimental and *ab initio* data used in the analysis (with their uncertainties), and of calculated "band constants" $\{G_v, B_v, D_v, H_v, \ldots\}$ of all 12 levels supported by our potentials, together with FORTRAN subroutines for calculating the recommended MLR and CPE potential energy functions, are provided in the supplementary material associated with this paper.[33]

TABLE V. Fitted term values and band constants (in cm^{-1}) determined for the $A\,^1\Pi_u$ state from the DPF analyses yielding our recommended MLR^{ab} and CPE model potentials. The band constants were obtained from fits using the recommended MLR^{ab} model. The effect of $A\,^1\Pi_u$-state Λ-doubling was neglected.

$v'(J')$	MLR^{ab}	CPE	$T_{v'}$	$B_{v'}$
2(0)			22 221.03 (6)	0.923 (8)
2(1)	22 222.878(49)	22 222.83		
2(2)	22 226.568(52)	22 226.53		
3(0)			22 877.72 (13)	0.880 (25)
3(1)	22 879.487(90)	22 879.44		
3(2)	22 883.001(80)	22 882.96		

IV. CONCLUDING REMARKS

The present work has determined improved empirical values of the fundamental properties of the beryllium dimer, together with analytic potential energy functions that predict all of the experimental data within their uncertainties and are fully differentiable across the whole real domain. These MLR^{ab} and CPE functions incorporate an optimal balance of flexibility and physical constraints, in that they readily incorporate the proper long-range behaviour, and implicitly include the ability to represent the unusual abrupt change in slope of the vibrational spacing plot at $v = 4$ (see Fig. 2 of Ref. 10). Although it is fully linear with respect to its parameters, the CPE potential required ∼1.5 times more fitting parameters than does the MLR function which is strongly nonlinear in parameter space, but incorporates the theoretical dispersion coefficients and damping functions explicitly. While the orthogonal polynomial form of the CPE potential energy function has many attractive features,[31,44] one weakness is its inability to provide reliable extrapolation behaviour at small distances, outside the data-sensitive region. The damping functions used in MLR potential were confirmed to be important for ensuring realistic behaviour of the short-range repulsive wall,[30] and in minimizing the number of required fitting parameters.

In very recent work, Sheng *et al.*[9] have presented an intuitively appealing explanation for the anomalous nature of the potential energy function of ground-state Be_2 with its "hairpin-bend" vibrational spacing plot. Their explanation is that we should think of the potential energy function for this system as a sum of two distinct components. The first is a simple van der Waals well due to the sum of attractive dispersion forces with a repulsive wall due to electrons in *s*-type orbitals, shown as a green short-dashed curve in Fig. 1. The second is a term due to *sp* mixing that weakens the repulsive wall, and hence acts as a "net attractive" term. Their model function for the sum of these two components[9] is shown as the green dotted curve in Fig. 1. As is evident there, their result disagrees significantly with both the present empirical functions and the *ab initio* points;[3,7,8] indeed its fit to the present experimental data set yielded $\overline{dd} = 132$, which is more than two orders of magnitude worse than those of our best models. However, it does seem to provide a gratifyingly plausible physical explanation for the anomalous nature of the Be_2 potential energy function.

In conclusion, the present study finds that empirical DPF analyses of the same spectroscopic + *ab initio* data set, using two completely different types of potential energy function models, yield potential energy curves that are completely equivalent. These empirical potentials predict that the equilibrium bond length of ground-state Be_2 is $r_e = 2.445(5)$ Å and its well depth is $\mathfrak{D}_e = 934.9(0.4)$ cm^{-1} (the average for our two models). These properties are remarkably close to the most recent *ab initio* estimates[8] 2.444(3) Å and 935(10) cm^{-1}, respectively, but the much smaller uncertainty of the present value for $\mathfrak{D}_e$ provides a residual challenge for further *ab initio* work on this system. Our predicted small positive values of its scattering length $a_S \approx 0.77$–0.90 Å reflect the fact that repulsion and attraction are almost balanced for a collision at

low kinetic energy. This leads to the prediction that the total elastic scattering cross section for colliding beryllium atoms will approach a very small value in the low temperature limit.

ACKNOWLEDGMENTS

The Canadian team is pleased to thank the Natural Sciences and Engineering Research Council of Canada for financial support of this project through provision of a "Discovery Grant" to R.J.L. The Moscow team is pleased to acknowledge the partial support for this project the Russian Foundation for Basic Researches (research Project No. 11-03-00307a). The U.S. group is grateful for support from the National Science Foundation *via* grant CHE-126556.

[1] J. M. L. Martin, Chem. Phys. Lett. **303**, 399 (1999).
[2] R. J. Gdanitz, Chem. Phys. Lett. **312**, 578 (1999).
[3] I. Röeggen and L. Veseth, Int. J. Quantum Chem. **101**, 201 (2005).
[4] V. Spirko, J. Mol. Spectrosc. **235**, 268 (2006).
[5] M. J. Jamieson, A. S.-C. Cheung, H. Ouerdane, G.-H. Jeung, and N. Geum, J. Phys. B: At. Mol. Opt. Phys. **40**, 3497 (2007).
[6] K. Patkowski, R. Podeszwa, and K. Szalewicz, J. Phys. Chem. A **111**, 12822 (2007).
[7] K. Patkowski, V. Spirko, and K. Szalewicz, Science **326**, 1382 (2009).
[8] J. Koput, Phys. Chem. Chem. Phys. **13**, 20311 (2011).
[9] X. W. Sheng, X. Y. Kuang, P. Li, and K. T. Tang, Phys. Rev. A **88**, 022517 (2013).
[10] J. M. Merritt, V. E. Bondybey, and M. C. Heaven, Science **324**, 1548 (2009).
[11] R. J. Le Roy, *Equilibrium Structures of Molecules*, edited by J. Demaison and A. G. Csaszar (Taylor and Francis, London, 2011), Chap. 6, pp. 159–203.
[12] S. G. Porsev and A. Derevianko, J. Exp. Theor. Phys. **102**, 195 (2006).
[13] J. A. Coxon, J. Mol. Spectrosc. **117**, 361 (1986).
[14] M. Gruebele, E. Keim, A. Stein, and R. J. Saykally, J. Mol. Spectrosc. **131**, 343 (1988).
[15] E. Tiemann, Z. Phys. D **5**, 77 (1987).
[16] E. Tiemann, Mol. Phys. **65**, 359 (1988).
[17] J. Y. Seto, Z. Morbi, F. Charron, S. K. Lee, P. F. Bernath, and R. J. Le Roy, J. Chem. Phys. **110**, 11756 (1999).
[18] P. G. Hajigeorgiou and R. J. Le Roy, J. Chem. Phys. **112**, 3949 (2000).
[19] J. Y. Seto, R. J. Le Roy, J. Vergès, and C. Amiot, J. Chem. Phys. **113**, 3067 (2000).
[20] C. Samuelis, E. Tiesinga, T. Laue, M. Elbs, H. Knöckel, and E. Tiemann, Phys. Rev. A **63**, 012710 (2000).
[21] A. Pashov, W. Jastrzębski, and P. Kowalczyk, Comput. Phys. Commun. **128**, 622 (2000).
[22] A. Pashov, W. Jastrzębski, and P. Kowalczyk, J. Chem. Phys. **113**, 6624 (2000).
[23] A. Grochola, W. Jastrzebski, P. Kowalczyk, P. Crozet, and A. J. Ross, Chem. Phys. Lett. **372**, 173 (2003).
[24] Y. Huang and R. J. Le Roy, J. Chem. Phys. **119**, 7398 (2003); **126**, 169904 (2007) (erratum).
[25] R. J. Le Roy, D. R. T. Appadoo, K. Anderson, A. Shayesteh, I. E. Gordon, and P. F. Bernath, J. Chem. Phys. **123**, 204304 (2005).
[26] R. J. Le Roy and R. D. E. Henderson, Mol. Phys. **105**, 663 (2007).
[27] B. M. Giuliano, L. Bizzocchi, and J.-U. Grabow, J. Mol. Spectrosc. **251**, 261 (2008).
[28] R. J. Le Roy, N. Dattani, J. A. Coxon, A. J. Ross, P. Crozet, and C. Linton, J. Chem. Phys. **131**, 204309 (2009).
[29] P. E. Bernath, Science **324**, 1526 (2009).
[30] R. J. Le Roy, C. C. Haugen, J. Tao, and H. Li, Mol. Phys. **109**, 435 (2011).
[31] L. Busevica, I. Klincare, O. Nikolayeva, M. Tamanis, R. Ferber, V. V. Meshkov, E. A. Pazyuk, and A. V. Stolyarov, J. Chem. Phys. **134**, 104307 (2011).
[32] H. Knöckel, S. Ruhmann, and E. Tiemann, J. Chem. Phys. **138**, 094303 (2013).
[33] See supplementary material at http://dx.doi.org/10.1063/1.4864355 for ASCII files containing listings of the data used in the present work, for tabulations of the vibrational energies and rotational constants of the $X\,^1\Sigma_u^+$ State of Be_2 generated from our final MLR potential, for Fortran subroutines for generating the recommended MLR and CPE potential energy functions, and for figures illustrating the determination and some properties of these selected PEC models.
[34] V. V. Meshkov, A. V. Stolyarov, and R. J. Le Roy, Phys. Rev. A **78**, 052510 (2008).
[35] These additional data were obtained from a re-examination of the original SEP laser scans by author M.H. (2012) that showed that a feature that had originally been (mis)interpreted as being the onset of the continuum[10] was actually the rising edge of a $v' = 11$ line.
[36] R. J. Le Roy, "Level 8.0: A computer program for solving the radial Schrödinger equation for bound and quasibound levels," University of Waterloo Chemical Physics Research Report CP-663, 2007; see http://leroy.uwaterloo.ca/programs/.
[37] R. J. Le Roy, J. Seto, and Y. Huang, "`DPotFit 2.0`: A computer program for fitting diatomic molecule spectra to potential energy functions," University of Waterloo Chemical Physics Research Report CP-667, 2013; see http://leroy.uwaterloo.ca/programs/.
[38] G. Audi, A. H. Wapstra, and C. Thibault, Nucl. Phys. A **729**, 337 (2003).
[39] W. H. Press, S. A. Teukolsky, W. T. Vetterling, and B. P. Flannery, *Numerical Recipes in Fortran 77* (Cambridge University Press, 1999).
[40] J. More, B. Garbow, and K. Hillstrom, MINPACK software for solving nonlinear equations and nonlinear least squares problems, University of Chicago, Argonne National Laboratory, 1999, see http://www.netlib.org/minpack.
[41] R. J. Le Roy, J. Mol. Spectrosc. **191**, 223 (1998).
[42] R. J. Le Roy, "Energy levels of a diatomic near dissociation," *Molecular Spectroscopy*, edited by R. N. Barrow, D. A. Long, and D. J. Millen (Chemical Society of London, 1973), Vol. 1, Chap. 3.
[43] A. A. Radzyg and B. M. Smirnov, *Reference Data on Atoms, Molecules and Ions* (Springer, Berlin-Heidelberg, 1985).
[44] J. C. Mason and D. C. Handscomb, *Chebyshev Polynomials* (CRC Press, 2003).
[45] At distances smaller than r_{min} the CPE potential could behave unphysically due to improper extrapolation of the polynomial expansion.
[46] J. Stärck and W. Meyer, Chem. Phys. Lett. **258**, 421 (1996).
[47] V. E. Bondybey, Chem. Phys. Lett. **109**, 436 (1984).